Scientific Research Publishing

Journal of Materials Science and Chemical Engineering, 2020, 8, 85-91
https://www.scirp.org/journal/msce
ISSN Online: 2327-6053
ISSN Print: 2327-6045

Single-Mode Fabry-Pérot Quantum Cascade Lasers at λ~10.5 μm

Shouzhu Niu[1], Junqi Liu[1,2,3], Jinchuan Zhang[1,2,3], Ning Zhuo[1,2,3], Shenqiang Zhai[1,2,3], Xiaohua Wang[1,2*], Zhipeng Wei[1,2]

[1]State Key Laboratory of High Power Semiconductor Lasers, School of Science, Changchun University of Science and Technology, Changchun, China
[2]Key Laboratory of Semiconductor Materials Science, Institute of Semiconductors, Chinese Academy of Sciences, Beijing, China
[3]Center of Materials Science and Optoelectronics Engineering, University of Chinese Academy of Sciences, Beijing, China
Email: *biewang2001@126.com

How to cite this paper: Niu, S.Z., Liu, J.Q., Zhang, J.C., Zhuo, N., Zhai, S.Q., Wang, X.H. and Wei, Z.P. (2020) Single-Mode Fabry-Pérot Quantum Cascade Lasers at λ~10.5 μm. *Journal of Materials Science and Chemical Engineering*, **8**, 85-91.
https://doi.org/10.4236/msce.2020.83007

Received: March 5, 2020
Accepted: March 16, 2020
Published: March 19, 2020

Abstract

In this paper, we report a single-mode Fabry-Pérot long wave infrared quantum cascade lasers based on the double phonon resonance active region design. For room temperature CW operation, the wafer with 35 stages was processed into buried heterostructure lasers. For a 4 mm long and 13 μm wide laser with high-reflectivity (HR) coating on the rear facet, continuous wave output power of 43 mW at 288 K and 5 mW at 303 K is obtained with threshold current densities of 2.17 and 2.7 kA/cm^2. The lasing wavelength is around 10.5 μm. Single mode emission was observed for this particular device over the whole investigated current and temperature range.

Keywords

Quantum Cascade Laser, Long Wave Infrared, Double Phonon Resonance

1. Introduction

In the last 20 years, quantum cascade lasers (QCLs) have received a great deal of attention because of their potential advantages for use in a wide range of areas, including infrared countermeasures, environmental monitoring, free-space optical communications, and optical gas sensing [1] [2] [3]. Among them, the long-wave infrared (LWIR, λ = 8 - 12 μm) QCLs are particularly important due to low atmosphere absorption loss and the rich variety of molecular species have their "fingerprint" absorption in this spectrum range [4]. To date, watt-level outputs at wavelengths in the middle-wave infrared (MWIR, λ = 3 - 5 μm) range have been obtained [5]. However, because of the limitation of the intrinsic tech-

nological characteristic of long-wave devices (such as increased free-electron optical losses at longer wavelengths, the lower intersubband gain, the decreased optical confinement), the progress of LWIR QCLs had been slower than the MWIR QCLs [6] [7] [8]. The room temperature continuous wave operation of LWIR QCL can be obtained by few groups [9] [10] [11]. Therefore, the further study on LWIR QCLs is necessary.

The first room temperature continuous wave LWIR QCLs was demonstrated using a double phonon resonance structure by Mattias Beck [12]. Base on the same design, continuous wave (CW) CW output power of 45 mW at 10˚C, wavelength ~9.4 μm have been demonstrated by Chuncai Hou [13]. However, the room temperature (RT) continuous wave (CW) operation of single mode LWIR QCL can be obtained by few groups, especially when the wavelength is longer than 10 μm.

In this letter, we present a single mode LWIR QCL with a continuous wave (CW) operating temperature up to 303 K. The active region is designed with a double phonon resonance and grown with strain-compensation technology. For a 4 mm long and 13 μm wide QCL with high-reflectivity (HR) coating on the rear facet, CW output power of 43 mW at 288 K and 5 mW at 303 K is obtained, at a lasing wavelength of ~10.5 μm.

2. Experimental Details

The 35 periods, double phonon resonance active region used is based on InGaAs/InAlAs material system, lattice-matched to InP and grown by molecular beam epitaxy (MBE). The active core structure presented in this paper is similar to Ref. 13. The complete structure includes several layers, include 4 μm lower InP cladding layer (Si, 3E16 cm^{-3}), 0.3-μm-thick n-$In_{0.53}Ga_{0.47}As$ layer (Si, 4E16 cm^{-3}), 35 active/injector stages, 0.3-μm-thick n-$In_{0.53}Ga_{0.47}As$ layer (Si, 4E16 cm^{-3}), 2.6 μm upper cladding layer (Si, 3E16 cm^{-3}), 0.15 μm gradually doped layer (changing from 1E17 to 3E17 cm^{-3}) and 0.8 μm highly doped cladding layer (Si, 5E18 cm^{-3}).

Then the wafer was processed in a narrow-stripe, buried heterostructure by photolithography and wet chemical etching. After etching, in order to confinement of carriers and improve radiation efficiency, the semi-insulating InP (Fe-doped) was grown by metal organic chemical vapor deposition (MOCVD). Next, a 450-nm thick SiO_2 layer was deposited by plasma enhanced chemical vapor deposition (PECVD) for electrical insulation, and Ti/Au layer was growthed by e-beam evaporation to realize the electrical contact. In order to reduce thermal resistance, an additional 5-μm-thick Au layer was subsequently electroplated. With thinning and annealing, the wafer was then cleaved into 4-mm-long laser bars and mounted epilayer side down on the copper heat sink with indium solder.

3. Results and Discussion

Figure 1(a) shows the optical power-current-voltage (PIV) characteristics for a 4

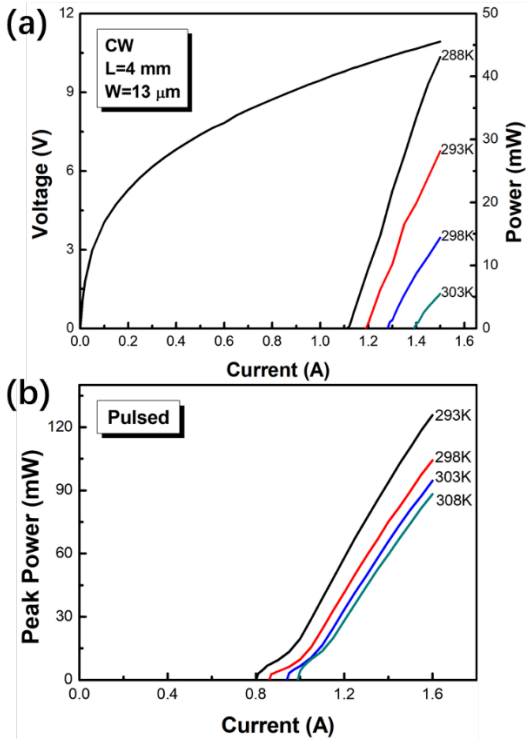

Figure 1. (a) Output optical power versus injection current of a 13 μm-wide and 4-mm long device in CW mode at different heat sink temperatures between 288 and 303 K along with V-I curves at 288 K. (b) Peak power of the laser changes with heat sink temperatures at the repetition frequency of 5 kHz and a pulse width of 2 μs.

mm long, 13 μm wide, buried heterostructure laser operating at different heat sink temperatures from 288 to 323 K. The output power was measured with a calibrated thermopile detector. At 288 K, CW threshold current density of ~2.17 kA/cm^2 was observed, and the laser exhibited optical output power of 43 mW and a slope efficiency dP/dI of 118 mW/A. When the temperature higher, the threshold current increased to ~2.7 kA/cm^2, and while still more than 5 mW of output power was emitted at 303K. The pulsed peak output power of 125 mW was obtained at 293 K with a repetition frequency of 5 kHz and a pulse width of 2 μs, while still more than 88 mW of output power was emitted at 308 K, as shown in **Figure 1(b)**. At 293 K, the threshold current of pulsed mode is 0.8 A (1.5 kA/cm^2). The slope efficiency of the device can be well calculated by the following model shown as equation:

$$\frac{dP}{dI} = \frac{h\nu}{e} N_p \frac{\alpha_m}{\alpha_W + \alpha_m} \eta_i \tag{1}$$

where $h\nu$ is the photon energy, e is the elemental electronic charge, N_p is number of cascade period, and η_i is the internal quantum efficiency of each period. According to this equation, the internal quantum efficiency is around 38% per cascade period at 288 K. The performance of the LWIR QCL shows good performance.

The spectrum characteristic of LWIR QCL is shown in **Figure 2**. The emission

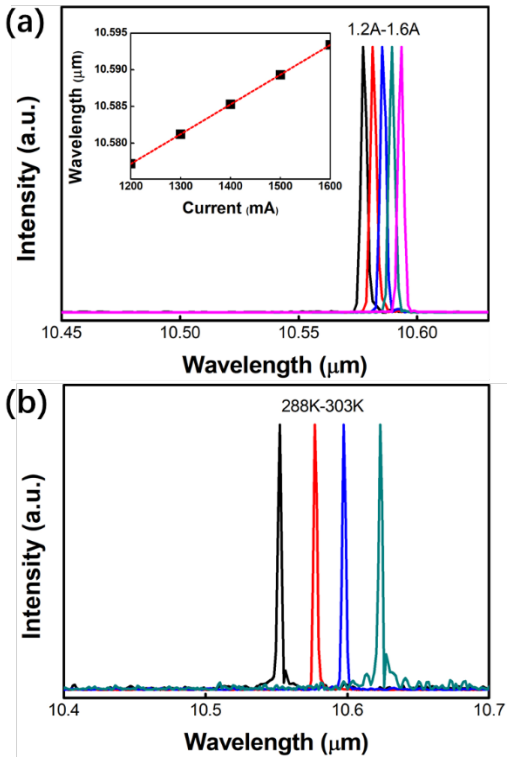

Figure 2. (a) CW lasing spectra at a different injection current from 1.2 to 1.6 A with a step of 0.1 A. The inset shows the linear-fit tuning characteristics of the lasing wavelength with electrical power for the same device. (b) CW emitting spectrum of QCL at different heat sink temperature between 288 and 303 K.

frequency ν of a QCL can be turned over a small range by changing the current and temperature. **Figure 2(a)** demonstrates the CW lasing spectra of the same device at different injection currents, from 1.2 to 1.6 A, with a step of 0.1 A at 293 K, the single mode frequency changes from 10.577 to 10.593 μm corresponding to the electrical power tuning coefficient $\Delta\nu/\Delta P$ of 2.8 nm/W. **Figure 2(b)** shows the normalized CW lasing spectra at a current of 1.02 I_{th} with temperature ranging from 288 to 303 K with a step of 5 K of the device. The single lasing mode frequency changes from 10.552 μm at 283 K to 10.623 μm at 303 K. The characteristic of a single mode is obvious in spite of no grating modulating the optical mode. This rather surprising fact can be explained by a small defect within the laser cavity, as indicated by an intensity modulation of the subthreshold Fabry-Perot fringes at twice the cavity mode spacing.

In order to investigate the thermal behavior, we measured the threshold current characteristic at the different heatsink temperatures in CW and pulsed mode shown in **Figure 3**. The red line fits with the exponential function $J_{th} = J_0\exp(T/T_0)$, where J_{th} is the threshold current density, J_0 is the constant and T_0 is the characteristic temperature. The T_0 is 132 K for the pulsed mode. Generally, due to the low heat conductivity of InGaAs/InAlAs ultrathin layer, the heat dissipation for the active region in CW operation mode is poor, thus the core temperature T_{act} of the QCL is much higher than the heatsink temperature T_{sink}. As a

result, the threshold current increases more rapidly with a higher value in CW mode than in pulsed mode as the temperature is increased. From 288 to 303 K, T_0 decreases to 71 K for CW mode. For high temperature and high power CW operation the lower threshold power density and weaker temperature dependence are required.

The far-field measurement was done by mounting the laser on a computer controlled rotational stage with a step resolution of 0.05˚. A room temperature operation HgCdTe detector was located 35 cm away from the QCL to collect the lasing light. **Figure 4** shows the measured lateral far-field radiation patterns of the LWIR QCL with the black dots and the fitted result of Gauss function with the red line. The measured full width at half maximum (FWHM) of the far-field pattern is 27.64˚, which can be explained by the diffraction limit formula $\sin\theta = 1.22\lambda/D$, where θ is the diffraction angle, λ is the lasing wavelength and D is the width of the waveguide.

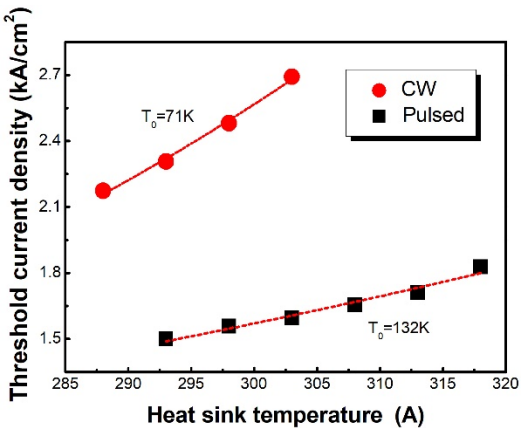

Figure 3. Threshold current density as a function of heat sink temperature in CW and pulsed mode of a 4-mm-long and 13-μm-wide LWIR QCL. The red dashed line is fitted with the exponential function $J_{th} = J_0\exp(T/T_0)$.

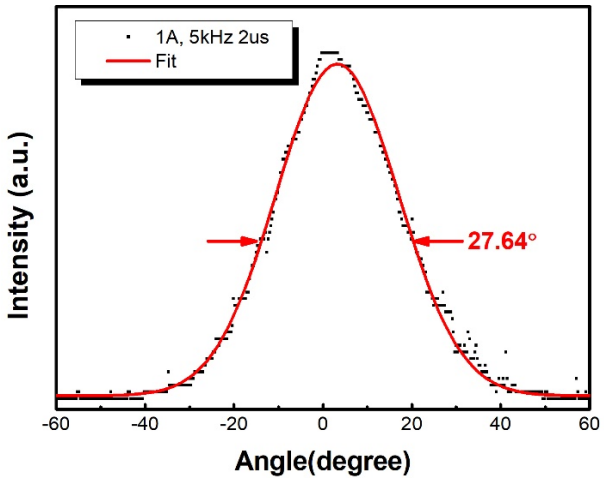

Figure 4. Measured lateral far-field radiation patterns for the devices at pulsed driving currents of 1 A under 5 kHz repetition frequency and 1% duty circle, the dot is the measurement and the red dashed line is the result fitted with the Gauss function.

4. Conclusion

In conclusion, a single mode QCL emitting at 10.5 μm has been demonstrated based on the double phonon resonance active region design. A CW output power of 43 mW was demonstrated at 288 K with a laser chip which has a 4-mm-long cavity and a 13-μm-wide stripe. The threshold current density is measured as 2.17 kA/cm^2 at 288 K and the far-field pattern shows normal single-lobed distribution. Single mode emission was observed for the device over the whole investigated current and temperature range, which shows a good potential for practical applications.

Acknowledgements

The authors would like to acknowledge Liang Ping and Hu Ying for their help with device fabrication.

This work is supported by the National Natural Science Foundation of China (Grant No. 61674021, 11674038, 61704011, 61904017), the Foundation of State Key Laboratory of High Power Semiconductor Lasers, the Youth Foundation of Changchun University of Science and Technology (Grant No. XQNJJ-2018-18).

Conflicts of Interest

The authors declare no conflicts of interest regarding the publication of this paper.

References

[1] Faist, J., Capasso, F., Sivco, D.L., Sirtori, C., Hutchinson, A.L. and Cho, A.Y. (1994) Quantum Cascade Laser. *Science*, **264**, 553-556. https://doi.org/10.1126/science.264.5158.553

[2] Razeghi, M., Bandyopadhyay, N., Bai, Y., Lu, Q. and Slivken, S. (2013) Recent Advances in Mid Infrared (3-5μm) Quantum Cascade Lasers. *Optical Materials Express*, **3**, 1872. https://doi.org/10.1364/OME.3.001872

[3] Vitiello, M.S., Scalari, G., Williams, B. and Natale, P.D. (2015) Quantum Cascade Lasers: 20 Years of Challenges. *Optics express*, **23**, 5167. https://doi.org/10.1364/OE.23.005167

[4] Troccoli, M., Lyakh, A., Fan, J., Wang, X., Maulini, R., Tsekoun, A.G., Go, R. and Patel, C.K.N. (2013) Long-Wave IR Quantum Cascade Lasers for Emission in the λ = 8-12μm Spectral Region. *Optical Materials Express*, **3**, 1546. https://doi.org/10.1364/OME.3.001546

[5] Bai, Y., Bandyopadhyay, N., Tsao, S., Slivken, S. and Razeghi, M. (2011) Room Temperature Quantum Cascade Lasers with 27% Wall Plug Efficiency. *Applied Physics Letters*, **98**, 181102. https://doi.org/10.1063/1.3586773

[6] Faist, J. (2007) Wallplug Efficiency of Quantum Cascade Lasers: Critical Parameters and Fundamental Limits. *Applied physics letters*, **90**, 253512. https://doi.org/10.1063/1.2747190

[7] Troccoli, M., Wang, X. and Fan, J. (2010) Quantum Cascade Lasers: High-Power Emission and Single-Mode Operation in the Long-Wave Infrared (>6 μm). *Optical Engineering*, **49**, 111106. https://doi.org/10.1117/1.3498778

[8] Yanga,Q.K., Schilling, C., Ostendorf, R., Hugger, S., Fuchs, F. and Wagner, J. (2012) Wall-Plug Efficiency of Mid-Infrared Quantum Cascade Lasers. *Journal of Applied Physics*, **111**, 053111. https://doi.org/10.1063/1.3692392

[9] Yu, J.S., Slivken, S., Evans, A. and Razeghi, M. (2008) High-Performance, Continuous-Wave Quantum-Cascade Lasers Operating up to 85˚C at λ~8.8 μm. *Applied Physics A*, **93**, 405. https://doi.org/10.1007/s00339-010-5873-z

[10] Baranov, A.N., Bahriz, M. and Teissier, R. (2016) Room Temperature Continuous Wave Operation of InAs-Based Quantum Cascade Lasers at 15 μm. *Optics express*, **24**, 18799. https://doi.org/10.1364/OE.24.018799

[11] Zhang, J., Wang, L., Zhang, W., Liu, W., Liu, J., Liu, F., Li, L and Wang, Z. (2011) Holographic Fabricated Continuous Wave Operation of Distributed Feedback Quantum Cascade Lasers at $\lambda\approx$8.5 μm. *Journal of Semicond*, **32**, 044008. https://doi.org/10.1088/1674-4926/32/4/044008

[12] Beck, M., Hofstetter, D., Aellen, T., Faist, J., Oesterle, U., Ilegems, M., Gini, E. and Melchior, H. (2002) Continuous Wave Operation of a Mid-Infrared Semiconductor Laser at Room Temperature. *Science*, **295**, 301. https://doi.org/10.1126/science.1066408

[13] Hou, C., Zhang, J., Zhai, S., Zhuo, N., Liu, J., Wang, L., Liu, S., Liu, F. and Wang, Z. (2011) Room Temperature Continuous Wave Operation of Quantum Cascade Laser at λ~9.4 μm. *Journal of Semicond*, **39**, 034001. https://doi.org/10.1088/1674-4926/39/3/034001